

*DRAFT*

**76295**  
Impact Melt Breccia  
260.7 grams



*Figure 1: Astronaut pushing rover uphill. Broken boulder at station 6, Apollo 17. Boulder tracks lead back up North Massif. NASA# AS-17-164-5954.*

**Introduction**

Sample 76295 was chipped from block 1 of the big boulder at station 6 (figure 1; Wolfe et al. 1981; Heiken et al. 1973; Meyer 1994). Tracks made by this broken

boulder show that it originated high up on the North Massif. The interpretation is that this boulder was part of the ejecta blanket from the gigantic impact that produced the Serenitatis Basin.



*Figure 2: Fresh broken surface of 76295, chipped off of block 1 of large boulder in figure 1. Scale is 1 cm. NASA# S72-56409.*

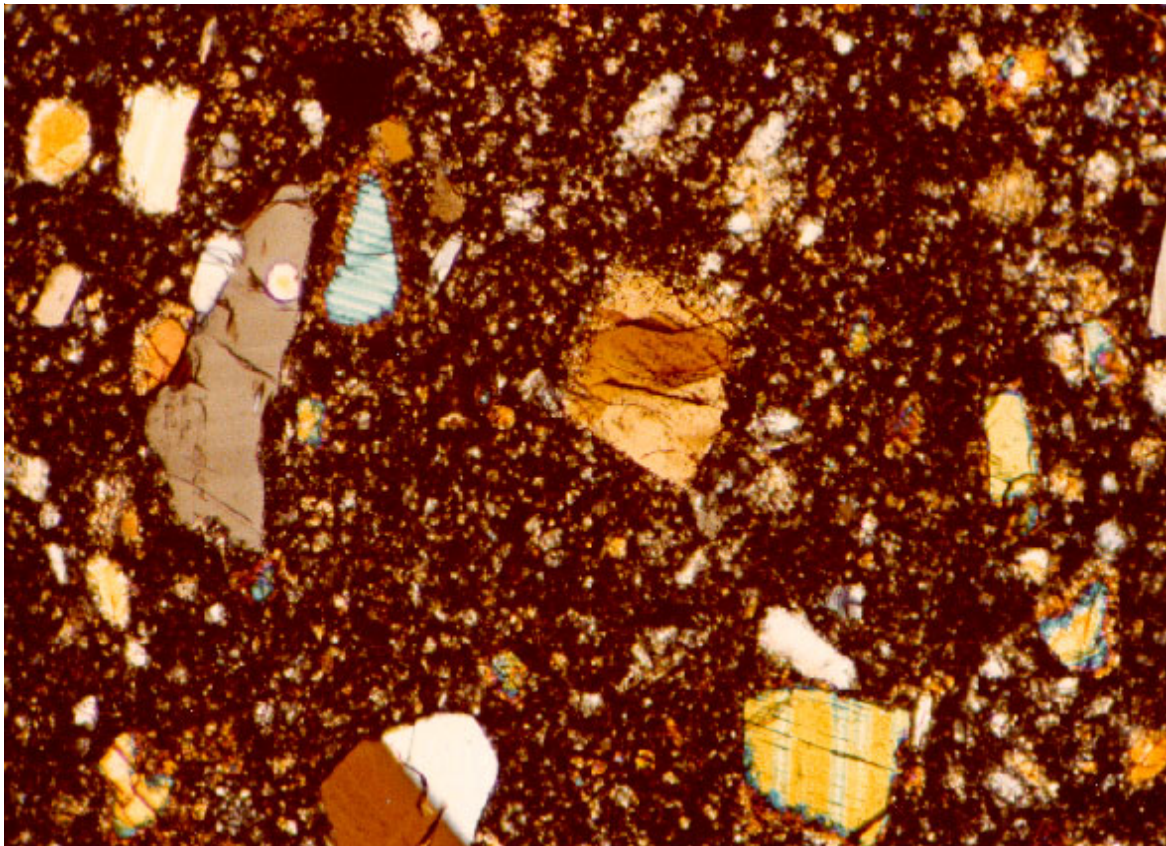


*Figure 3: Photomicrograph of thin section (crossed Nicols) illustrating mineral clasts in matrix of 76295. Scale: field of view is 1.4 mm. NASA# S79-27273*

This important boulder was observed to be made of three lithologic units (76295 is from unit C). 76295 is a non-vesicular, crystalline matrix breccia with a blue-grey color (similar to 76275). Light and dark clasts have a distinct outline with the matrix (figure 2). The B1 surface has zap pits, while the N1 surface is freshly broken. The other surfaces of the rock were covered with a “buff powder” and/or “patina” (Heiken et al. 1973).

The fine grain texture and overall clast/matrix texture of 76295 and 76275 were important evidence for the thermal model developed by Simonds (1975) and Onorato et al. (1976) for the genesis of impact melt breccias. Briefly, this model is that hot impact melt entrained, and was quickly cooled, by cold clastic debris that was partially digested. The resulting melt sheet then crystallized to a fine grain matrix including undigested mineral and lithic clasts.

### **Petrography**

Sample 76295 has been described by Heiken et al. (1973) and Simonds (1975) as a fine subophitic impact

melt. It is a banded, clast-bearing, nonvesicular, blue-grey breccia with aphanitic matrix. The blue-grey breccia matrix contains bands and swirls of minor (~10%) tan matrix breccia and partially dissolved mineral and rock clasts. A slab sawn from the breccia (12) and the other saw cuts illustrates the “marbled” texture of the tan and blue-grey breccia matrix (figure 11). Four individual rock clasts have been studied by Simonds (1975).

Dark grey: Subophitic melt rock similar to matrix. Table 1, figure 7.

Light grey: Poikilitic melt rock similar to 76015. Table 1, figure 7.

Porous Basalt Clast: Similar to a basalt clast in 76015. Simonds (1975) Table 1, figures 5, 7.

Troctolite Clast (feldspathic olivine norite): Monomict breccia. Simonds (1975), Phinney (1981) Figure 6.

The matrix of 76295 is holocrystalline with only minor void space. The mode is about 50% plagioclase and 40% pyroxene with minor ilmenite, olivine and other

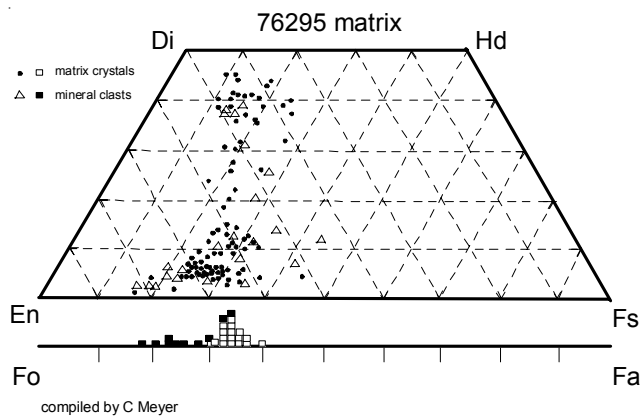


Figure 4: Composition of pyroxene and olivine in matrix of 76295 (data replotted from Phinney 1981).

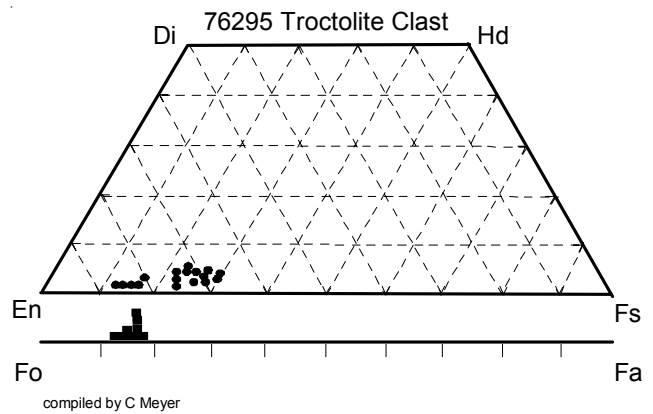


Figure 6: Composition of pyroxene and olivine in troctolite clast of 76295 (data replotted from Phinney 1981).

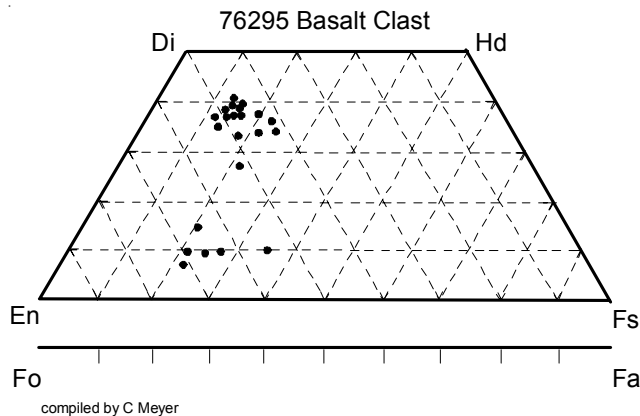


Figure 5: Composition of pyroxene and olivine in basalt clast within 76295 (data replotted from Phinney 1981).

minerals. Grain size of matrix feldspar is <15 microns, pyroxene 10-25 microns.

Norman et al. (1993) have compared the compositions of minerals in LKFM clasts in 76295 with minerals in similar clasts in 76315 and conclude that the clast population in 76295 is dominated by “Mg-suite norites, troctolites and gabbronorites”. Minor-element abundances in both olivine and pyroxene are unlike those found in lunar rocks of the ferroan anorthosite suite.

## Mineralogy

**Olivine:** Olivine is generally Fo<sub>67-78</sub> (Norman et al. 1993; Simonds 1975).

**Pyroxene:** The composition of pyroxene and olivine is shown in figure 4 – 6.

**Plagioclase:** Plagioclase is generally in the range of An<sub>81-97</sub> (Norman et al. 1993)

**Zircon:** Meyer found one large rounded zircon in the matrix of 76295.

**Metal:** Misra et al. (1976) studied the nickel-iron particles in 76295.

## Chemistry

The chemical composition of the blue-grey and tan matrix portions of 76295 were found to be identical (table 1; figure 7). Unpublished data can be found in Simonds and Warner (1981) and Phinney (1981). Higuchi and Morgan (1975) found that the matrix samples of 76295 were tightly grouped within meteorite group 2 on an Ir-Au-Re diagram, but that clasts extracted from 76295 had different ratios (figure 8).

### Mineralogical mode:

	Matrix	Basalt clast	Troctolitic clast
Plagioclase	50 %	50	50
Pigeonite	34	10	32
Augite	7	30	1
Olivine	7	0	17
Ilmenite	1	10	1

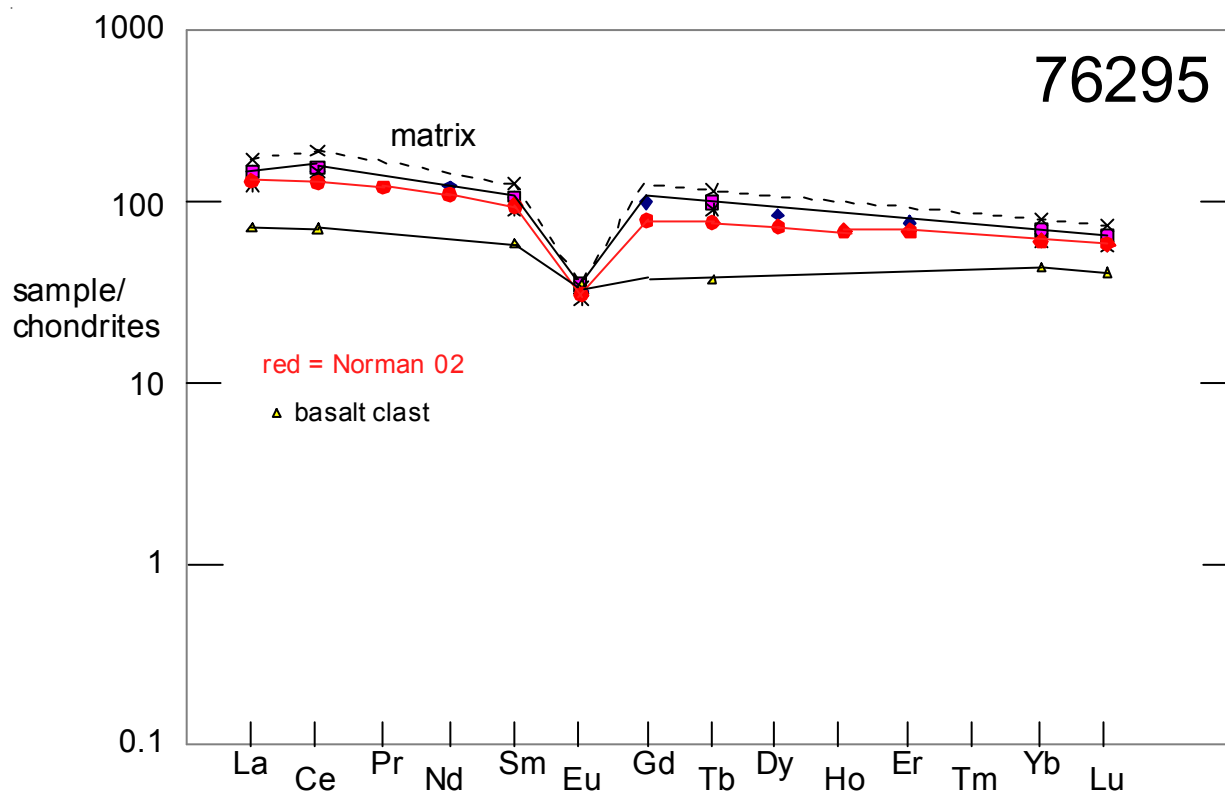


Figure 7: Normalized rare-earth-element composition diagram for matrix and clasts in 76295 (see table 1 for source of data).

The composition determined for the porous basalt clast was “unusual”.

*Note: there appears to a mistake in the tabulation of data from Higuchi and Morgan (1975) for 76295 matrix in Simonds (1975).*

### **Radiogenic age dating**

Cadogan and Turner (1976) determined the crystallization age of two samples of 76295 by the  $^{39}\text{Ar}$ - $^{40}\text{Ar}$  plateau technique. The tan matrix yielded an intermediate temperature plateau age of  $3.95 \pm 0.04$  b.y., and the blue grey matrix yielded and age of  $3.96 \pm 0.04$  b.y. However, both sub-samples exhibited appreciable decreases in  $^{40}\text{Ar}$  over the last 30% high-temperature release (figure 9).

Unpublished elemental and isotopic data for U, Th and Pb by Leon Silver and Rb-Sr by Larry Nyquist were reported in Phinney (1981).

A zircon in 76295 has been dated at  $\sim 4200$  b.y. by the ion probe method (Pigeon et al. 2003, personal communication).

### **Cosmogenic isotopes and exposure ages**

Data from radiation counting is given in Heiken et al. (1973) (table 3). Unpublished isotopic data for He, Ne, Ar, Kr and Xe by as determined by Bogard are found in Phinney (1981).

### **Other Studies**

Gose et al. (1978) propose that the large scatter of magnetization direction of 76295 implies the predominance of pre-impact magnetization in this sample. Brecher (1976) makes convincing argument that alignment of magnetization follows the direction of foliation and is caused by “textural remanent magnetization”.

### **Processing**

Sample 76295 was one of the samples studied by the Station 6 Boulder Consortium led by Bill Phinney. A detailed guidebook of the results of this consortium is available from the Curator (Phinney 1981). Lithological maps of the boulders and of the samples are presented in a Tech Report by Heiken et al. (1973). The sketch in figure 10 shows the approximate location of the saw cuts for initial processing of 76295. The map of slab (,12) reproduced in figure 11 shows the

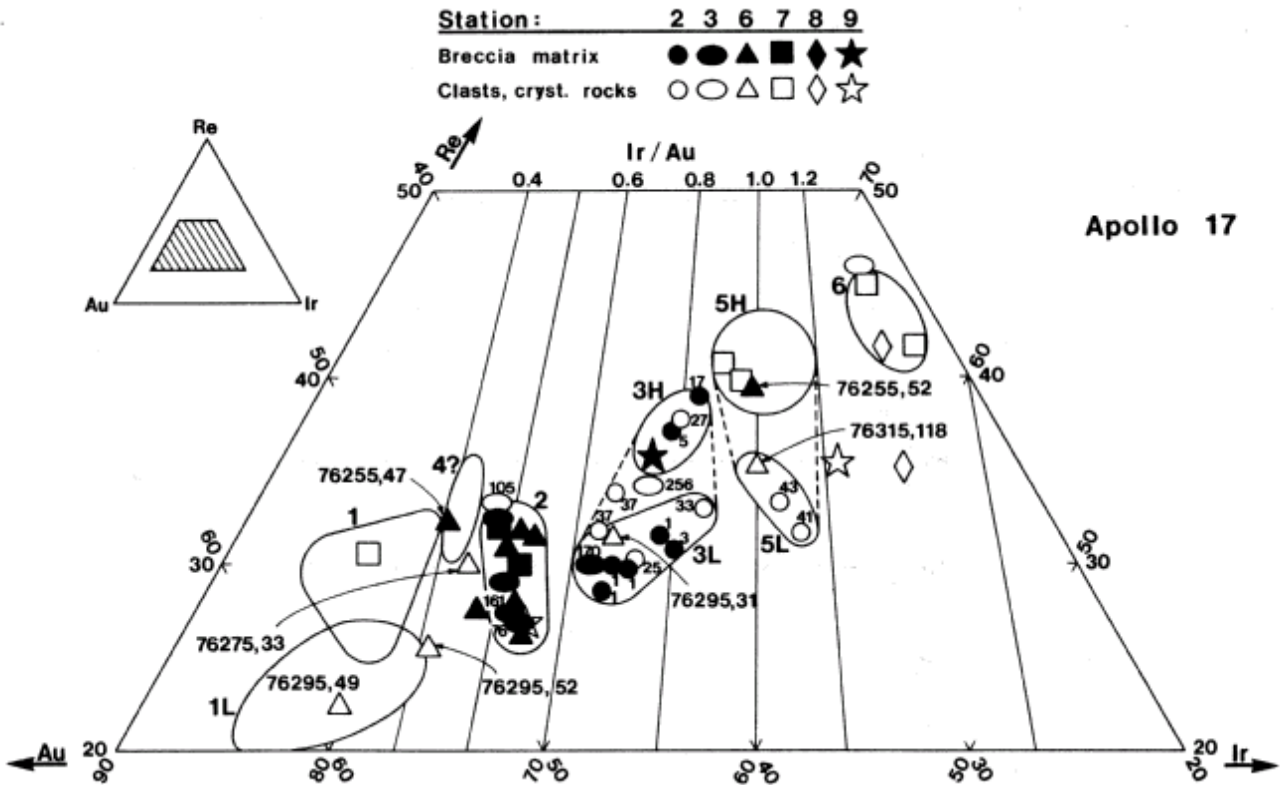


Figure 8: Composition diagram for three trace elements (Ir, Au and Re) showing tight grouping for matrix, but dispersed grouping for clasts in 76295 (figure from Higuchi and Morgan 1975).

tan lithology is surrounded by the more abundant blue-grey lithology.

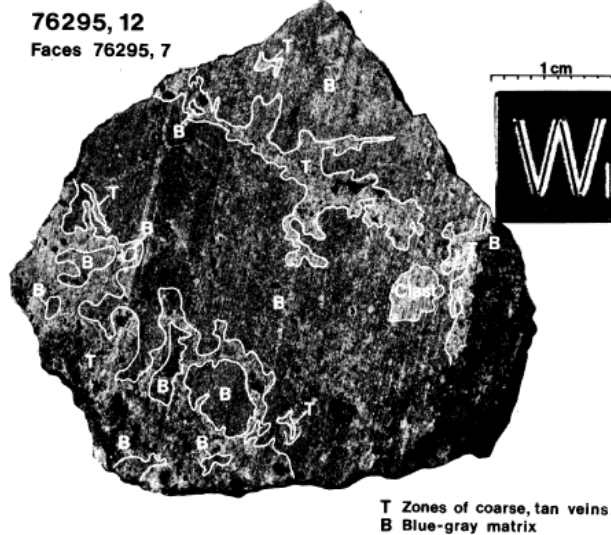


Figure 11: Map of slab through 76295 showing marbled texture of blue-grey and tan matrix (from Phinney et al. 1981).

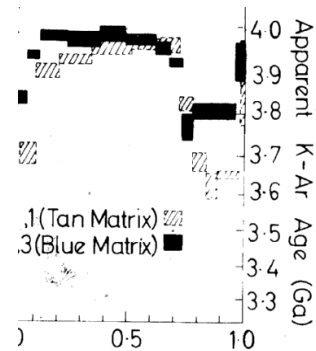


Figure 9: Ar<sup>39</sup>-Ar<sup>40</sup> release diagram for two matrix samples of 76295 (from Cadogan and Turner 1976).

**List of Photos #**

- S72-56406-56411 PET mug shots
- S74-18439-18446 saw cuts
- S74-20186-20190 group photos
- S74-20819
- S77-26955
- S79-27270-27274 thin section photos

**Table 1a. Chemical composition of 76295.**

<i>reference weight</i>	Simonds 75 blue matrix	Higuchi 75 blue matrix	Phinney 81 tan matrix	Higuchi 75 tan matrix	Phinney 81 basalt clast	Higuchi 75 basalt clast	Wiesmann 75 basalt clast	Phinney 81 dark grey	Phinney 81 light grey
SiO <sub>2</sub> %	47.03	(a)	47.55	(d)	48.11	(d)		46.89	47.04
TiO <sub>2</sub>	1.39	(a)	1.64	(d)	1.8	(d)	1.85	(b) 1.5	1.36
Al <sub>2</sub> O <sub>3</sub>	18.25	(a)	17.67	(d)	16.95	(d)		18.67	18.98
FeO	9.09	(a)	9.05	(d)	9.17	(d)		8.79	8.44
MnO									
MgO	10.78	(a)	9.78	(d)	9.72	(d)		9.66	9.64
CaO	11.54	(a)	11.49	(d)	11.22	(d)		11.69	11.95
Na <sub>2</sub> O	0.76	(a)	0.74	(d)	0.75	(d)		0.71	0.66
K <sub>2</sub> O	0.26	(a)	0.29	(d)	0.6	(d)		0.23	0.28
P <sub>2</sub> O <sub>5</sub>	0.32	(a)							
S %	0.06	(a)							
<i>sum</i>									
Sc ppm			17.8	(e)	21	(e)		18.2	16.7
V									
Cr			1382	(e)	1440	(e)	1364	(b) 1440	1360
Co			19.9	(e)	24.9	(e)		28	23.1
Ni		250	(c) 160	(e) 218	(c) 230	(e) 146	(c)	203	179
Cu									
Zn		27.1	(c) 20	(e) 2.5	(c)	2.2	(c)	2.6	2.3
Ga									
Ge ppb		316	(c)	374	(c)	321	(c)	423	198
As									
Se		103	(c)	132	(c)	235	(c)	68	75
Rb	5.43	(b) 9.2	(c)	4.22	(c)	12.5	(c) 20.47	(b) 1.75	3.31
Sr	175	(b)					191	(b)	
Y									
Zr	541	(b)					232	(b)	
Nb									
Mo									
Ru									
Rh									
Pd ppb									
Ag ppb		4.55	(c)	5.09	(c)	1.03	(c)	1.2	0.87
Cd ppb		6.56	(c)	1	(c)	1.13	(c)	1.28	1.88
In ppb									
Sn ppb									
Sb ppb		393	(c)	1.68	(c)	1.84	(c)	2.11	1.03
Te ppb		4.9	(c)	4.62	(c)	5.81	(c)	1.9	2.4
Cs ppm		0.151	(c)	0.297	(c)	0.649	(c)	0.11	0.192
Ba	376	(b)					334	(b)	
La	37.8	(b)	37.5	(e)	22	(e)	18.2	(b) 44.2	31.8
Ce	95.7	(b)	102	(e)	59	(e)	46.6	(b) 127	95.8
Pr									
Nd	60	(b)					31.1	(b)	
Sm	16.9	(b)	17	(e)	10.9	(e)	9.22	(b) 20.4	14.3
Eu	1.91	(b)	2.11	(e)	2.15	(e)	2.08	(b) 2.01	1.77
Gd	21.3	(b)					12.4	(b)	
Tb			3.91	(e)	2.72	(e)		4.56	3.56
Dy	22.3	(b)					13.3	(b)	
Ho									
Er	13.2	(b)					8.06	(b)	
Tm									
Yb	12	(b)	12.2	(e)	8.8	(e)	7.6	(b) 14.1	10.8
Lu			1.71	(e)	1.31	(e)	1.07	(b) 1.95	1.49
Hf			13.2	(e)	7.9	(e)		16.3	12.4
Ta			1.9	(e)	1.4	(e)		2.4	1.7
W ppb									
Re ppb		0.566	(c)	0.486	(c)	0.267	(c)	0.456	0.48
Os ppb									
Ir ppb		7.88	(c)	6.1	(c)	3.18	(c)	5.42	5.98
Pt ppb									
Au ppb		4.36	(c)	3.43	(c)	2.91	(c)	3.93	2.65
Th ppm	6.12	(b)	5.6	(e)	2.2	(e)	2.01	(b) 7.6	5.2
U ppm	1.83	(b) 1.9	(c)	1.32	(c)	0.76	(c) 0.66	(b) 1.94	1.62

*technique (a) XRF, (b) IDMS, (c) RNAA, (d) fused bead, (e) INAA*

**Table 1b. Chemical composition of 76295.**

<i>reference</i>	Norman 02	
<i>weight</i>	3 g	
SiO <sub>2</sub> %	46.4	(b)
TiO <sub>2</sub>	1.49	(b)
Al <sub>2</sub> O <sub>3</sub>	18.2	(b)
FeO	8.39	(b)
MnO	0.12	(b)
MgO	10.5	(b)
CaO	11.2	(b)
Na <sub>2</sub> O	0.71	(b)
K <sub>2</sub> O	0.34	(b)
P <sub>2</sub> O <sub>5</sub>		
S %		
<i>sum</i>		
Sc ppm	18.4	(a)
V	45	(a)
Cr	1325	(a)
Co	26.4	(a)
Ni	208	(a)
Cu	11.6	(a)
Zn	14	(a)
Ga	5.3	(a)
Ge ppb		
As		
Se		
Rb	7.5	(a)
Sr	183	(a)
Y	132	(a)
Zr	587	(a)
Nb	37.7	(a)
Mo		
Ru ppb	10.5	(c )
Rh		
Pd ppb	11	(c )
Ag ppb		
Cd ppb		
In ppb		
Sn ppb		
Sb ppb		
Te ppb		
Cs ppm	0.29	(a)
Ba	378	(a)
La	33.3	(a)
Ce	84.7	(a)
Pr	11.7	(a)
Nd	53.8	(a)
Sm	15.2	(a)
Eu	1.85	(a)
Gd	16.8	(a)
Tb	3	(a)
Dy	19	(a)
Ho	4.1	(a)
Er	11.7	(a)
Tm		
Yb	10.5	(a)
Lu	1.53	(a)
Hf	11.8	(a)
Ta	1.6	(a)
W ppb	920	(a)
Re ppb	0.56	(c )
Os ppb		
Ir ppb	5.61	(c )
Pt ppb	12.3	(c )
Au ppb		
Th ppm	6.41	(a)
U ppm	1.64	(a)

*technique* (a) ICP-MS, (b) fused bead elec. Probe, (c ) ICP-MS with isotope dilution

**Table 2. Light and/or volatile elements for 76295.**

reference weight	Simonds 75 blue matrix	Higuchi 75 blue matrix	Phinney 81 tan matrix	Higuchi 75 tan matrix	Phinney 81 basalt clast	Higuchi 75 basalt clast	Wiesmann 75 basalt clast	Phinney 81 dark grey	Phinney 81 light grey
Li ppm	19.4	(b)					20.5	(b)	
Be									
B		Phinney 1981							
C		105							
S		731							
F ppm									
Cl									
Br ppb		78.7	(c)	27.9	(c)	30.5	(c)	37.5	23.5
I									
Pb ppm									
Hg ppb									
Tl		1.41	(c)	0.64	(c)	0.99	(c)	0.33	0.44
Bi		0.97	(c)	0.8	(c)	0.4	(c)	0.56	0.46

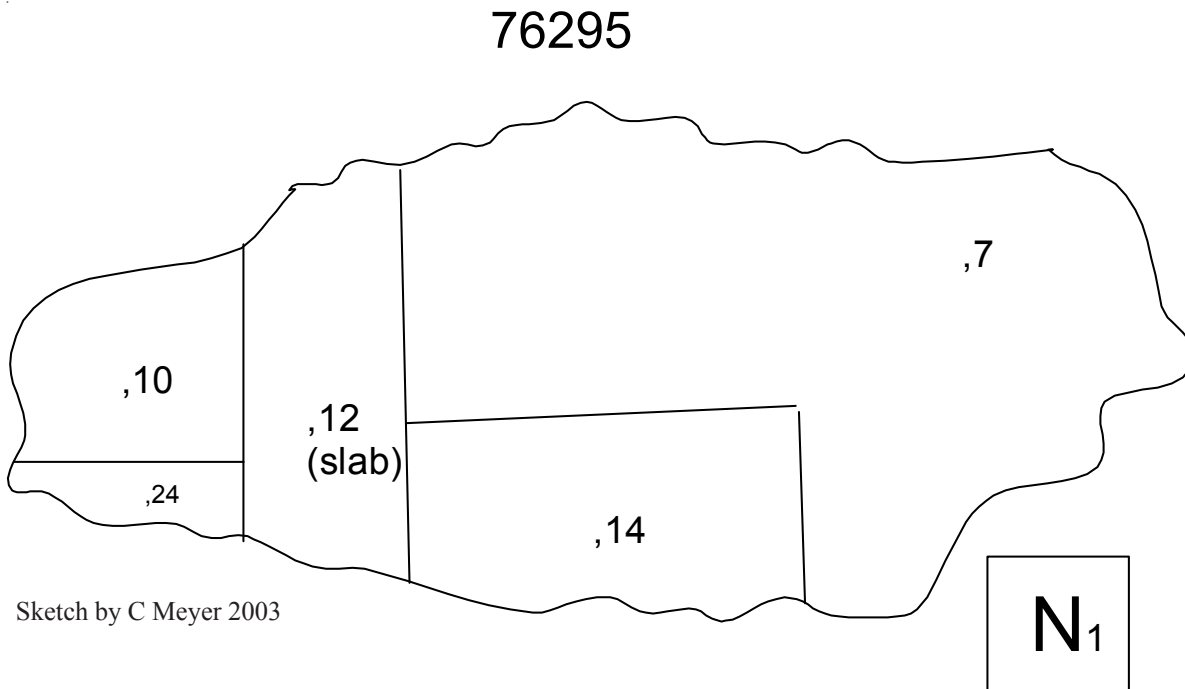


Figure 10: Initial saw cuts of 76295 (compare with figure 2).

**Table 3: Radiation Counting for 76295.**

	Oak Ridge	Battelle
Th ppm	5.4	5.76
U ppm	1.5	1.55
K %	0.227	0.23
26Al	67	71
22Na	54	64
54Mn	38	70
56Co	41	35
46Sc	5	6.4
48V		
69Co		< 1.2

as reported in Heiken et al. 1973